




# Polarization measurements of deep- to extreme-ultraviolet high harmonics generated in liquid flat sheets

VÍT SVOBODA,<sup>1,3</sup> ZHONG YIN,<sup>1,4</sup>  TRAN TRUNG LUU,<sup>1,2</sup>  AND HANS JAKOB WÖRNER<sup>1,5</sup> 

<sup>1</sup>Laboratory of Physical Chemistry, ETH Zürich, 8093 Zürich, Switzerland

<sup>2</sup>Department of Physics, The University of Hong Kong, Hong Kong SAR, China

<sup>3</sup>vit.svoboda@phys.chem.ethz.ch

<sup>4</sup>yinz@ethz.ch

<sup>5</sup>hwoerner@ethz.ch

**Abstract:** Laboratory-based coherent light sources enable a wide range of applications to investigate dynamical processes in matter. High-harmonic generation (HHG) from liquid samples is a recently discovered coherent source of extreme-ultraviolet (XUV) radiation potentially capable of achieving few-femtosecond to attosecond pulse durations. However, the polarization state of this light source has so far remained unknown. In this work, we characterize the degree of polarization of both low- and high-order harmonics generated from liquid samples using linearly polarized 400 nm and 800 nm drivers. We find a remarkably high degree of linear polarization of harmonics ranging all the way from the deep-ultraviolet (160 nm) across the vacuum-ultraviolet into the XUV domain (73 nm). These results establish high-harmonic generation in liquids as a promising alternative to conventional sources of XUV radiation, combining the benefits of high target densities comparable to solids with a continuous sample renewal that avoids the limitations imposed by laser-induced damage.

© 2021 Optical Society of America under the terms of the [OSA Open Access Publishing Agreement](#)

## 1. Introduction

Coherent light sources in the extreme-ultraviolet spectral range have become a popular tool to investigate fundamental properties of matter. They have enabled remarkable discoveries across many scientific fields [1–6]. Yet, the majority of those sources are embedded in large-scale research facilities such as free-electron laser or synchrotron facilities. Recent advances in high-harmonic generation provide an alternative avenue towards coherent XUV light sources which can be realized in the laboratory-based environment [7–12]. Moreover, HHG is inherently delivering few-femtosecond to attosecond pulse durations, thereby opening unique possibilities to investigate dynamical processes with unprecedented time resolution in addition to the selectivity provided by the XUV to soft-X-ray wavelengths.

Since the early pioneering work [13,14], HHG from gas targets has evolved into a widespread laboratory-based source of XUV radiation to study chemical dynamics in real time. A main disadvantage of the conventionally used gas targets is their low photon flux. Development of HHG from solids [15–20] has overcome this limitation by providing higher conversion efficiency [21]. However, laser-induced damage of the solid target limits the repetition rate and incident laser intensity, thus restricting their practical significance as light sources. Liquid samples combine the advantages of gaseous and solid HHG targets, i.e. they merge continuous sample renewal with high target densities, potentially achieving higher photon fluxes.

Early work by DiChiara et al. [22] reported harmonic generation limited to the visible spectral range from liquid H<sub>2</sub>O and D<sub>2</sub>O by mid-IR lasers using a 27 cm long fluid column. One experimental challenge in extending this work to the XUV was the creation of a stable liquid

sheet in a vacuum environment. The field of liquid-phase HHG has been enabled by the recent development of the flat-jet technique [23–26]. This allows one to deliver a liquid sample into a vacuum environment in the form of a thin sheet of liquid; both of these conditions are essential for a successful detection of high harmonics in the XUV spectral range. Recently, the first experimental demonstration of XUV harmonics from liquids has been realized by Luu et al. [26], with its recent extension to the regime of few-cycle drivers [27]. However, the polarization state of these harmonics has remained unknown so far.

Here, we describe the first polarization measurements of high harmonics from liquids. We studied water and alcohols (ethanol and 2-propanol) at two different driving wavelengths (400 nm and 800 nm) and different linear polarization configurations (either s or p). A four-mirror rotating in-vacuum XUV polarizer is used to characterize the polarization state of the emitted harmonics from the deep-ultraviolet (DUV) (160 nm) into the XUV (73 nm). Our measurements reveal a remarkably high degree of polarization, i.e. larger than about 95% in all studied cases. This observation is similar to HHG in atomic gases driven by linearly polarized laser fields, where no evidence of depolarization was found [28–30]. However, it contrasts with the observation of significant depolarization in HHG from atomic clusters [31]. Experimental evidence of depolarization has also been found in polarization measurements of HHG emitted from solid samples [32]. The origin of the effect was attributed to intraband dynamics, but it was mentioned that other mechanisms may contribute to depolarization as well [32]. The experimental observations of depolarization in clusters [31] and solids [32] therefore raises the interesting question whether or to what extent HHG emission from liquid samples is depolarized.

This paper is organized as follows: Section 2 describes the experimental setup and the data-acquisition procedure. Section 3 presents the results of the polarization measurement and discusses the main experimental observations in terms of the molecular character of the liquids and the effect of the flow rate. The conclusions are presented in Section 4. The appendix introduces the metrics of the polarization measurements using the four-mirror polarizer.

## 2. Experimental setup

Polarization measurements were conducted with multi-cycle laser pulses centered at 800 nm or 400 nm, generating high-order harmonics from water, ethanol and 2-propanol. In the experiment, schematically depicted in Fig. 1, laser pulses from an amplified titanium:sapphire system with a duration of around 30 fs and a 1 kHz repetition rate were used. In the case of the 800 nm driver, the input beam was passed through a zero-order optically-contacted half-wave plate ( $\lambda/2$ , EKSMO Optics) centered at 800 nm with an anti-reflection (AR) coating to set the polarization of the input beam to be either s- or p-polarized. The linear polarization of the input beam was measured to be  $|S_1| \geq 0.99$  following a rotating quarter-wave-plate method described by Schaefer et al. [33] using a Glan-Taylor polarizing cube with an extinction ratio of  $10^5:1$  and a zero-order optically-contacted quarter-wave plate ( $\lambda/4$ ) centered at 800 nm with an AR coating. After the half-wave plate, the input beam was focused using a silver-coated spherical concave mirror ( $f = 400$  mm) and was coupled into an interaction chamber through a 1-mm-thick UV fused-silica window. A pulse energy of 0.8 mJ was measured in front of the vacuum chamber. In the case of the 400 nm driver, the p-polarized input beam was frequency-doubled in a 300  $\mu\text{m}$  thick  $\beta$ -barium borate (BBO) crystal with 20 % conversion efficiency to get 0.16 mJ s-polarized 400 nm pulses. Afterwards, the beam passed a zero-order AR-coated optically-contacted  $\lambda/2$  plate centered at 400 nm. The linear polarization of the beam was measured to be  $|S_1| \geq 0.98$  using the same method as in the 800 nm case. The 400 nm beam was focused by an aluminium spherical concave mirror ( $f = 400$  mm) through the same window as in the 800-nm case.

The interaction chamber hosted a custom-built flat-jet setup. A pair of glass nozzles ( $\sim 50$   $\mu\text{m}$  orifice diameter) formed a liquid sheet with  $\sim 1$   $\mu\text{m}$  thickness [26]. The sheet was oriented such that its normal vector was parallel to the input beam. The liquid from the flat jet was collected in

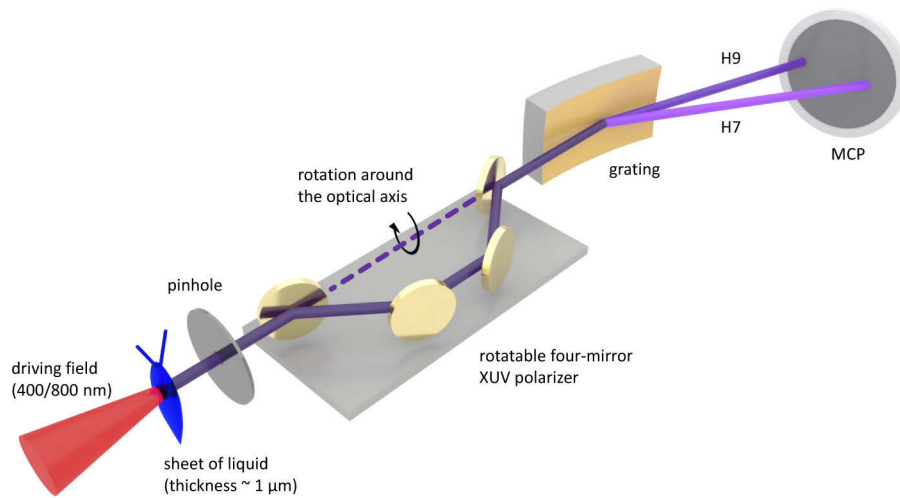


**Fig. 1.** Schematic drawing of the experimental setup. An input beam (either 800 nm or 400 nm) was focused into the interaction chamber hosting a flat-jet setup (formed by colliding two cylindrical jets emanating from 50  $\mu\text{m}$  glass nozzles). High harmonics were generated by focusing the input beam on the thin ( $\sim 1 \mu\text{m}$ ) liquid sheet and were further propagated to a spectrometer chamber through a pinhole. The polarization state of individual harmonics was analyzed by a four-mirror rotating polarizer placed before a diffraction grating. The diffracted harmonics were detected using a combination of a position-sensitive detector (MCP) and a CCD camera (not shown).

a cold trap placed  $\sim 20$  cm downstream of the liquid sheet to maintain the vacuum necessary for negligible absorption of the generated XUV light.

The high-harmonic radiation entered the spectrometer chamber through a small pinhole allowing for differential pumping between the interaction and spectrometer chambers. The resulting pressure difference was at least two orders of magnitude. The spectrometer chamber hosted a four-mirror rotating in-vacuum polarizer, a diffraction grating, and a micro-channel-plate (MCP) detector backed with a phosphor screen. The polarizer was placed in front of the diffraction grating and allowed for an analysis of the Stokes parameters  $S_0$ ,  $S_1$ , and  $S_2$  of the individual harmonics (their definition is given in the [Appendix](#)). It consisted of four unprotected gold mirrors, each mounted at a grazing angle of incidence of  $20^\circ$ . The four mirrors were mounted on a common plate that could be rotated around the axis of the incoming beam by a stepper motor, reaching a nominal angular resolution of  $0.07^\circ$ . For additional details about the polarizer, see Ref. [20]. The commercial diffraction grating (Shimadzu 30-006, 300 lines/mm,  $3^\circ$  incidence angle) diffracted individual harmonics onto the position-sensitive MCP detector read out by an optical charge-coupled-device (CCD) camera.

A polarization measurement typically consisted of 540 steps ( $2^\circ/\text{step}$ ) evenly distributed over three full rotations of the polarizer. For each step, ten images were recorded with an integration time of 10 ms. These images were averaged and the static background was subtracted prior to further analysis. The Stokes parameters for each harmonic were analyzed using Eq. (5) (see [Appendix](#)) and the degree of polarization was calculated using Eq. (6). Since one polarizer is not enough to obtain the Stokes parameter  $S_3$ , we are not able to directly characterize any contribution of unpolarized harmonic radiation. However, the measured extinction ratio for all harmonics was always consistent with the one calculated for our polarizer. Thus, no evidence of depolarization has been observed.

### 3. Results and discussion

We investigated the polarization state of the harmonics generated from three different liquids: water, ethanol, and 2-propanol, to study the possible influence of their different electronic structures on the HHG process. We moreover compared 800 nm and 400 nm driving laser pulses to look for possible differences in the polarization state of the high harmonics that could be expected to appear as a consequence of varying relative contributions from different mechanisms. We also studied the influence of the flow rate on the polarization of high harmonics because an increase in the flow rate leads to a stretching of the flat sheet in both the vertical and horizontal directions, which changes the small, but non-vanishing curvature of the sheet. Finally, we compared the effect of s- and p-polarized driving pulses because the curvature of the flat sheet is stronger along the horizontal than along the vertical direction. In the remainder of the paper, s-polarized means a polarization direction parallel to the flow direction of the flat jet, see Fig. 1.

Exemplary data are shown in Fig. 2 for the s-polarized 800 nm driver and liquid water (flow rate of 5.3 mL/min). Panel A shows an image recorded for 10 ms at the polarizer angle  $\alpha = 0^\circ$  which should correspond to the intensity maximum of s-polarized harmonics as follows from Eq. (5). The image shows four strong harmonics (H5 - blue, H7 - red, H9 - yellow, and H11 - purple) and two much weaker harmonics (H13 and H15). The low-energy part of the image shows three additional weak signals, corresponding to harmonics (H7, H9, and H11, labelled 1, 2, and 3, respectively) observed in the second diffraction order ( $m = 2$ ) of the grating.

Panel B is a false-color representation of a polarization scan in which each horizontal line was obtained by integration of the signal from the camera image at a given angle along the vertical direction. The angle of the polarizer  $\alpha$  is changed from  $-360^\circ$  to  $720^\circ$  in  $2^\circ$  steps. All harmonics showed similar behaviour when the polarizer was rotated, meaning that they had similar polarization states. The intensity change with polarizer angle has a regular pattern of alternating intensity maxima and minima with one of the intensity maxima at  $\alpha = 0^\circ$  and the period of  $(180 \pm 2)^\circ$ . Following Eq. (5), this pattern is characteristic of s-polarized light. Our results thus show that an s-polarized driver leads to s-polarized harmonics. In the remaining analysis, we only focus on the strongest harmonics (H5, H7, H9, and H11) and refer to them as *main harmonics*.

In panel C, integrated intensities of the main harmonics are plotted as functions of the polarizer angle  $\alpha$ . The intensity maxima and minima are clearly visible with a high contrast ratio lying between 50 and 190, depending on the harmonic order. The fluctuation of the intensity maxima, expressed as a relative deviation, is about 4 %, reflecting a high stability of the flat jet over the entire polarization scan.

Panel D summarizes two methods used to calculate the degree of polarization of each main harmonic. In a simple approach (black), the intensity maxima and minima from panel C can be used. Following Höchst et al. [34], the degree of polarization can be defined as

$$D_{P,\text{simple}} = \frac{I_{\text{max}} - I_{\text{min}}}{I_{\text{max}} + I_{\text{min}}}, \quad (1)$$

where  $I_{\text{max}}$  and  $I_{\text{min}}$  are the intensity maximum and minimum for a given harmonic order, respectively. For all main harmonics, high values of the degree of polarization  $D_{P,\text{simple}} \geq 0.97$  are obtained. This is a reflection of the high contrast ratio as visible from panel C.

A more elaborate approach (blue line) defines the degree of polarization as in Eq. (6) via the evaluation of the Stokes parameters according to Eq. (5). In this approach, an error of the degree of polarization can be calculated using the error propagation law from the standard errors of the Stokes parameters  $S_0$ ,  $S_1$ , and  $S_2$  obtained from the non-linear fit to the intensity profiles in panel C.

The two approaches give consistent results. Both of them predict a high degree of polarization of the main harmonics; however the simple approach (black line) provides consistently lower

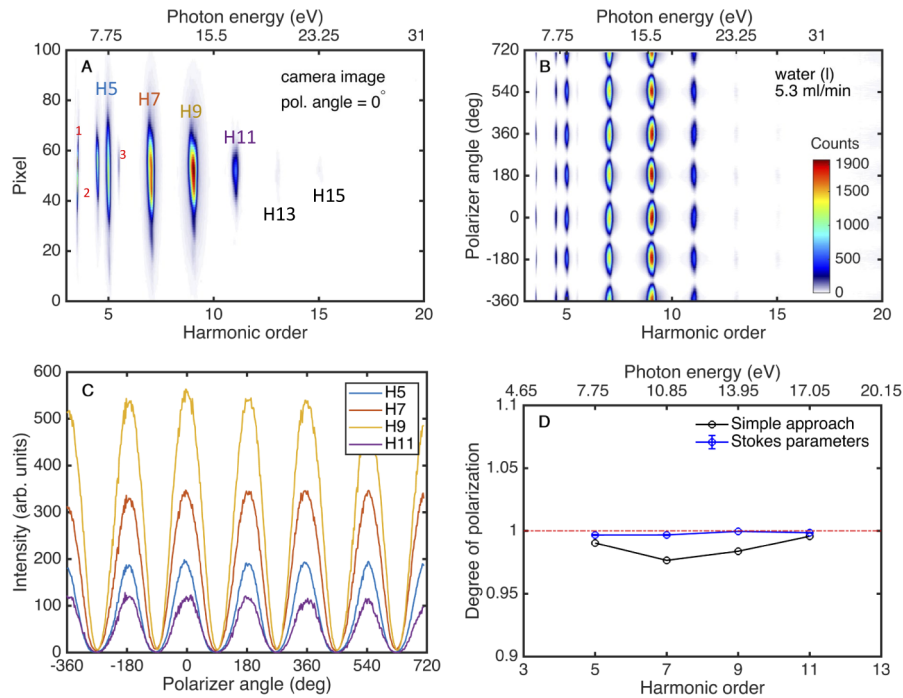


**Fig. 2.** Exemplary polarization measurement. Data are for harmonics generated in liquid water with an s-polarized 800 nm driving field. Panel A shows a camera image with several harmonics at one particular angle of the polarizer. Harmonics diffracted into the second order ( $m = 2$ ) of the grating are indicated by red numbers (1, 2, and 3). Panel B represents a polarization scan in which each horizontal line corresponds to a harmonic spectrum at a given polarizer angle. Panel C is a plot of integrated intensities of the harmonics H5, H7, H9, and H11 as a function of the polarizer angle. Panel D presents the results of two approaches to analyze the degree of polarization of selected harmonics. For more details, see the main text.

degrees of polarization due to its sensitivity to intensity fluctuations. The approach based on the evaluation of Stokes parameters (blue line) gives almost completely linearly polarized main harmonics,  $D_p \approx 1$ .

The Stokes parameters for the main harmonics are summarized in Table 1 as well as the resulting degree of polarization. All main harmonics are almost perfectly s-polarized with Stokes parameters  $|S_1| \geq 0.995$  and a negligibly small contribution of Stokes parameter  $S_2$ . This confirms that the s-polarized driver generates s-polarized harmonics in the liquid. In addition, the degree of polarization does not appear to depend on the harmonic order, at least within the studied energy range between 7.8 eV and 17.1 eV.

So far, we have been discussing one particular case of high harmonics generated from liquid water using a s-polarized 800 nm driver. To get deeper insight into the polarization of high harmonics generated in liquids, it is instructive to study several effects which may play a role. In particular, we have focused on: a) the driver wavelength (400 nm or 800 nm), b) a different polarization (s or p) of the driver, c) different liquids, and d) the flow rate of the flat jet.

We first discuss the effect of a different polarization (s or p) of the 800 nm driver. The resulting degrees of polarization based on the Stokes parameters for individual main harmonics generated in liquid water (flow rate 4.5 mL/min) are summarized in Fig. 3 in green. Panels A and B show the degree of polarization for p- and s-polarized 800 nm drivers, respectively. In both cases, the

**Table 1. The Stokes parameters and the degree of polarization for the main harmonics generated from liquid water using s-polarized 800 nm driver. HO stands for harmonic order,  $S_0$ ,  $S_1$ , and  $S_2$  are the Stokes parameters, and  $D_P$  is the degree of polarization with its standard error ( $2\sigma$ ).**

Water (l), s-polarized 800 nm driver					
HO	Photon energy (eV)	$S_0$	$S_1$	$S_2$	$D_P$
5	7.8	1	-0.995	0.052	$0.997 \pm 0.001$
7	10.9	1	-0.997	0.013	$0.997 \pm 0.001$
9	14.0	1	-0.996	-0.083	$1.000 \pm 0.001$
11	17.1	1	-0.996	-0.066	$0.999 \pm 0.001$

main harmonics are almost perfectly linearly polarized with  $D_P \approx 1$ , adopting the polarization direction of the driver. This means that highly polarized harmonics can be prepared irrespective of the linear polarization (s- or p-) of the 800 nm driver, at least in the energy range between 7.8 eV and 17.1 eV. Similar results were obtained for the 400 nm driver, see the green lines in Fig. 3 panels C and D. This further extends the previous conclusion that highly polarized harmonics from liquids can be prepared irrespective of the linear polarization (s vs. p) and wavelength (800 nm vs. 400 nm) of the driver.

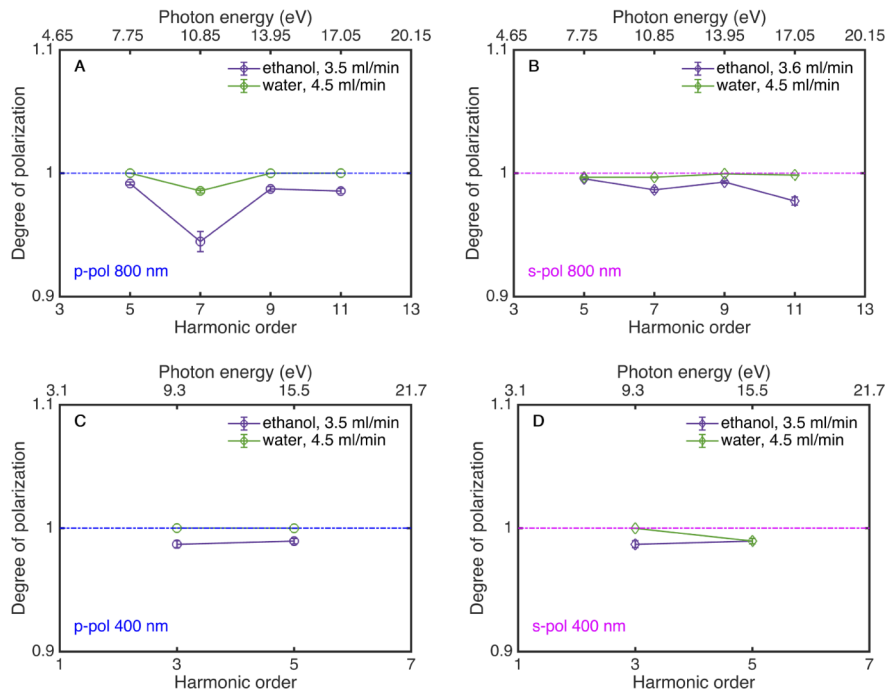


**Fig. 3.** Polarization state of harmonics generated from different liquids. Two different liquids are compared: ethanol (purple) and water (green). The flow rates are selected such that they provide the most stable flat jet. Panels A and B show the degree of polarization of the main harmonics generated from a p- or s-polarized 800 nm driver, respectively. Panels C and D show the same information for a 400 nm driver. For more details, see the main text.

Next, we discuss the effect of different liquids used to generate the harmonics. For a comparison, ethanol and water have been selected, representing prototypical liquids with different chemical

and physical properties. Figure 3 shows the results for 800 nm (panels A and B) and 400 nm (panels C and D) drivers. The degree of polarization of the harmonics generated in ethanol is slightly lower than of those generated in water, irrespective of the driver polarization or wavelength, see panels A - D. However, the same harmonics generated in ethanol display a high degree of polarization with  $D_p \geq 0.95$  in all studied cases. Thus, we can conclude that the polarization of the harmonics generated in liquids does not strongly depend on the nature of the liquid (water vs. ethanol).

We now discuss the effect of the flow rate on the polarization of the harmonics. We have performed these experiments only for ethanol and 2-propanol, since the liquid sheet of water is only stable in a narrower range of flow rates compared to the selected alcohols. Figure 4 shows the results for three different flow rates of ethanol (panels A and B) and 2-propanol (panels C and D): 3.0 mL/min, 3.5 mL/min, and 4.5 mL/min; all of these flow rates form a stable liquid sheet for both alcohols. Up to experimentally insignificant variations, the degree of polarization does not depend on the flow rate of the liquid, at least for the two studied alcohols.

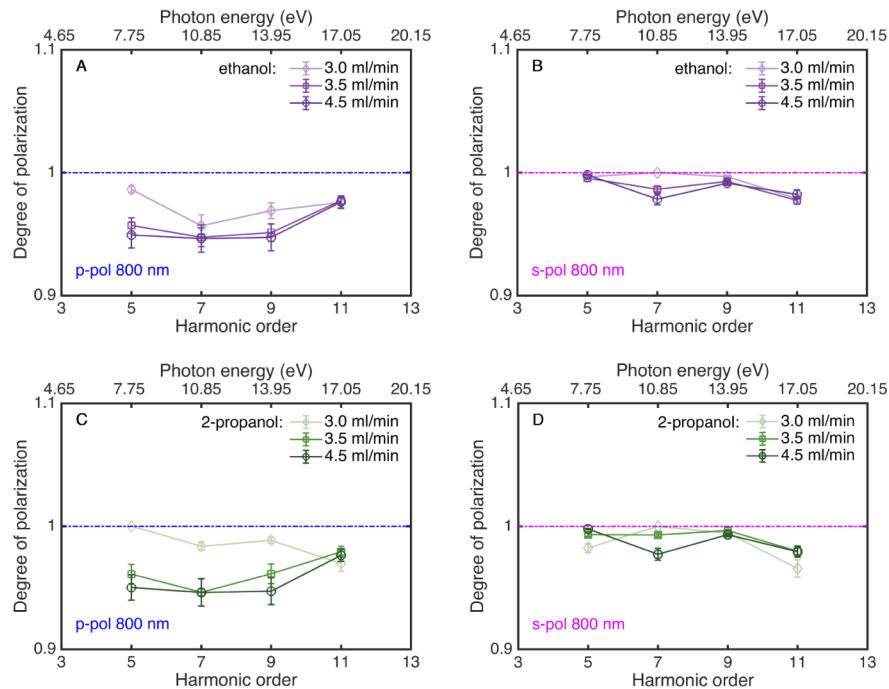


**Fig. 4.** Flow-rate dependence of the degree of polarization. Three different flow rates: 3.0 mL/min, 3.5 mL/min, and 4.5 mL/min are presented and compared for two liquids: ethanol (purple) and 2-propanol (green). Panels A and C and panels B and D show the degrees of polarization of the main harmonics generated from a p- or s-polarized 800 nm driver, respectively. For more details, see the main text.

#### 4. Conclusion

In the present work, we have performed polarization measurements of harmonics generated from thin flat sheets of different liquids from the DUV into the XUV. In summary, we have investigated several effects which may play a role in the harmonic-generation process and thus influence the degree of polarization of these harmonics. In particular, we have measured three different liquids (ethanol, 2-propanol, and water) using both s- or p-polarized 400 nm and 800 nm drivers and have studied the effect of the flow rate on the polarization. Interestingly, our results show that all

harmonics generated from liquids have a very high degree of polarization, reaching values close to unity, and can be made both s- or p-polarized depending on the polarization of the driver. We experimentally verified that the degree of polarization seems to be practically independent of the nature of the liquid, as well as its flow rate, at least for the studied harmonic energies between 7.8 eV and 17.1 eV. Our results open a wide range of applications for these liquid-generated harmonics since they provide a coherent and highly polarized light source in the DUV-XUV range, which can be expected to become a promising alternative to traditional sources for applications ranging from coherent diffractive imaging, over femto- and attosecond-time-resolved spectroscopies to XUV coherence tomography.

### Appendix: polarization measurements of XUV radiation

The polarization state of light can be characterized using the Stokes parameters forming a vector  $\mathbf{S} = (S_0, S_1, S_2, S_3)^T$ , where  $S_0$  describes the total intensity,  $S_1$  describes the linear s- or p-polarized light,  $S_2$  describes the linear  $\pm 45^\circ$  polarized light, and  $S_3$  describes the circularly polarized light [33]. The simplest polarization measurement in the XUV spectral range can be performed using a combination of a four-mirror polarizer and an intensity detector [34]. It can be shown that the Stokes vector  $\mathbf{S}_f$  for a beam exiting the polarizer is given as [35]

$$\mathbf{S}_f = \mathbf{R}(-\alpha)\mathbf{M}\mathbf{R}(\alpha)\mathbf{S}_i, \quad (2)$$

where  $\mathbf{R}(\alpha)$  is the rotational matrix

$$\mathbf{R}(\alpha) = \begin{pmatrix} 1 & 0 & 0 & 0 \\ 0 & \cos(2\alpha) & \sin(2\alpha) & 0 \\ 0 & -\sin(2\alpha) & \cos(2\alpha) & 0 \\ 0 & 0 & 0 & 1 \end{pmatrix} \quad (3)$$

describing the rotation of the polarizer through angle  $\alpha$ ,  $\mathbf{M}$  is the Müller matrix for the polarizer [36,37]

$$\mathbf{M} = 0.5 \begin{pmatrix} r_p^2 + r_s^2 \\ r_p^2 - r_s^2 \\ 2r_p r_s \cos(\psi) \\ 2r_p r_s \sin(\psi) \end{pmatrix} \cdot \begin{pmatrix} 1 & -\cos(2\psi) & 0 & 0 \\ -\cos(2\psi) & 1 & 0 & 0 \\ 0 & 0 & \sin(2\psi) \cos(\Delta) & \sin(2\psi) \sin(\Delta) \\ 0 & 0 & -\sin(2\psi) \sin(\Delta) & \sin(2\psi) \cos(\Delta) \end{pmatrix}, \quad (4)$$

in which  $\Delta = \delta_p - \delta_s$  is the total phase retardation and  $\psi = \arctan(r_p/r_s)$  depends on real reflectances  $r_{p,s}$ . Finally  $\mathbf{S}_i$  is the Stokes vector of the incident XUV light.

The detector is only measuring the intensity of the emerging beam as a function of the polarizer angle. Assuming that the polarizer has a large reflectivity difference between s- and p-polarized light, we can get the final form of the intensity function as

$$S_{0,f} = 0.5(S_{0,i} - S_{1,i} \cos(2\alpha) - S_{2,i} \sin(2\alpha)). \quad (5)$$

Nevertheless, a combination of one polarizer and a detector is not sufficient to measure all four Stokes parameters of the incident beam; but only the linear part of the Stokes vector



$\mathbf{S} = (S_0, S_1, S_2)^T$ . In such a situation, the degree of (linear) polarization is defined as [35]

$$D_P = \frac{\sqrt{S_{1,i}^2 + S_{2,i}^2}}{S_{0,i}}. \quad (6)$$

If the Stokes parameters are normalized to unit intensity, the degree of polarization has values between  $0 \leq D_P \leq 1$  where  $D_P = 1$  signifies completely linearly polarized light.

**Funding.** Eidgenössische Technische Hochschule Zürich (SEED-12 19-1/1-004952-000); European Research Council (772797).

**Acknowledgments.** The authors thank Andreas Schneider and Mario Seiler for their contributions to the construction and improvements of the experimental setup.

**Disclosures.** The authors declare no conflicts of interest.

**Data availability.** Data underlying the results presented in this paper are not publicly available at this time but may be obtained from the authors upon reasonable request.

## References

1. S. Eisebitt, J. Lüning, W. Schlotter, M. Lörger, O. Hellwig, W. Eberhardt, and J. Stöhr, "Lensless imaging of magnetic nanostructures by x-ray spectro-holography," *Nature* **432**(7019), 885–888 (2004).
2. H. N. Chapman, A. Barty, M. J. Bogan, S. Boutet, M. Frank, S. P. Hau-Riege, S. Marchesini, B. W. Woods, S. Bajt, W. H. Benner, R. A. London, E. Plönjes, M. Kuhlmann, R. Treusch, S. Düsterer, T. Tschentscher, J. R. Schneider, E. Spiller, T. Möller, C. Bostedt, M. Hoener, D. A. Shapiro, K. O. Hodgson, D. van der Spoel, F. Burmeister, M. Bergh, C. Caleman, G. Hultdt, M. M. Seibert, F. R. N. C. Maia, R. W. Lee, A. Szöke, N. Timneanu, and J. Hajdu, "Femtosecond diffractive imaging with a soft-x-ray free-electron laser," *Nat. Phys.* **2**(12), 839–843 (2006).
3. R. Schneider, T. Mehringer, G. Mercurio, L. Wenthaus, A. Classen, G. Brenner, O. Gorobtsov, A. Benz, D. Bhatti, L. Bocklage, B. Fischer, S. Lazarev, Y. Obukhov, K. Schlage, P. Skopintsev, J. Wagner, F. Waldmann, S. Willing, I. Zaluzhnyy, W. Wurth, I. A. Vartanyants, R. Röhlberger, and J. von Zanthier, "Quantum imaging with incoherently scattered light from a free-electron laser," *Nat. Phys.* **14**(2), 126–129 (2018).
4. M. Beye, S. Schreck, F. Sorgenfrei, C. Trabant, N. Pontius, C. Schüßler-Langeheine, W. Wurth, and A. Föhlisch, "Stimulated x-ray emission for materials science," *Nature* **501**(7466), 191–194 (2013).
5. S. Pathak, L. M. Ibele, R. Boll, C. Callegari, A. Demidovich, B. Erk, R. Feifel, R. Forbes, M. Di Fraia, L. Giannessi, C. S. Hansen, D. M. P. Holland, R. A. Ingle, R. Mason, O. Plekan, K. C. Prince, A. Rouzée, R. J. Squibb, J. Tross, M. N. R. Ashfold, B. F. E. Curchod, and D. Rolles, "Tracking the ultraviolet-induced photochemistry of thiophenone during and after ultrafast ring opening," *Nat. Chem.* **12**(9), 795–800 (2020).
6. T. Mazza, A. Karamatskou, M. Ilchen, S. Bakhtiarzadeh, A. Rafipoor, P. O'Keeffe, T. Kelly, N. Walsh, J. Costello, M. Meyer, and R. Santra, "Sensitivity of nonlinear photoionization to resonance substructure in collective excitation," *Nat. Commun.* **6**(1), 6799 (2015).
7. T. Popmintchev, M.-C. Chen, D. Popmintchev, P. Arpin, S. Brown, S. Ališauskas, G. Andriukaitis, T. Balčiūnas, O. D. Mücke, A. Pugzlys, A. Baltuška, B. Shim, S. E. Schrauth, A. Gaeta, C. Hernández-García, L. Plaja, A. Becker, A. Jaron-Becker, M. M. Murnane, and H. C. Kapteyn, "Bright coherent ultrahigh harmonics in the keV x-ray regime from mid-infrared femtosecond lasers," *Science* **336**(6086), 1287–1291 (2012).
8. S. M. Teichmann, F. Silva, S. Cousin, M. Hemmer, and J. Biegert, "0.5-keV soft x-ray attosecond continua," *Nat. Commun.* **7**(1), 11493–11496 (2016).
9. T. Gaumnitz, A. Jain, Y. Pertot, M. Huppert, I. Jordan, F. Ardana-Lamas, and H. J. Wörner, "Streaking of 43-attosecond soft-x-ray pulses generated by a passively CEP-stable mid-infrared driver," *Opt. Express* **25**(22), 27506–27518 (2017).
10. Y. Pertot, C. Schmidt, M. Matthews, A. Chauvet, M. Huppert, V. Svoboda, A. Von Conta, A. Tehlar, D. Baykusheva, J.-P. Wolf, and H. J. Wörner, "Time-resolved x-ray absorption spectroscopy with a water window high-harmonic source," *Science* **355**(6322), 264–267 (2017).
11. A. D. Smith, T. Balciunas, Y.-P. Chang, C. Schmidt, K. Zinchenko, F. B. Nunes, E. Rossi, V. Svoboda, Z. Yin, J.-P. Wolf, and H. J. Wörner, "Femtosecond soft-x-ray absorption spectroscopy of liquids with a water-window high-harmonic source," *J. Phys. Chem. Lett.* **11**(6), 1981–1988 (2020).
12. J. Li, J. Lu, A. Chew, S. Han, J. Li, Y. Wu, H. Wang, S. Ghimire, and Z. Chang, "Attosecond science based on high harmonic generation from gases and solids," *Nat. Commun.* **11**(1), 2748 (2020).
13. A. McPherson, G. Gibson, H. Jara, U. Johann, T. S. Luk, I. A. McIntyre, K. Boyer, and C. K. Rhodes, "Studies of multiphoton production of vacuum-ultraviolet radiation in the rare gases," *J. Opt. Soc. Am. B* **4**(4), 595 (1987).
14. M. Ferray, A. L'Huillier, X. F. Li, L. A. Lompre, G. Mainfray, and C. Manus, "Multiple-harmonic conversion of 1064 nm radiation in rare gases," *J. Phys. B* **21**(3), L31–L35 (1988).
15. S. Ghimire, A. D. DiChiara, E. Sistrunk, P. Agostini, L. F. DiMauro, and D. A. Reis, "Observation of high-order harmonic generation in a bulk crystal," *Nat. Phys.* **7**(2), 138–141 (2011).
16. T. T. Luu, M. Garg, S. Y. Kruchinin, A. Moulet, M. T. Hassan, and E. Goulielmakis, "Extreme ultraviolet high-harmonic spectroscopy of solids," *Nature* **521**(7553), 498–502 (2015).

17. G. Vampa, T. Hammond, N. Thiré, B. Schmidt, F. Légaré, C. McDonald, T. Brabec, and P. Corkum, "Linking high harmonics from gases and solids," *Nature* **522**(7557), 462–464 (2015).
18. O. Schubert, M. Hohenleutner, F. Langer, B. Urbanek, C. Lange, U. Huttner, D. Golde, T. Meier, M. Kira, S. W. Koch, and R. Huber, "Sub-cycle control of terahertz high-harmonic generation by dynamical Bloch oscillations," *Nat. Photonics* **8**(2), 119–123 (2014).
19. N. Yoshikawa, T. Tamaya, and K. Tanaka, "High-harmonic generation in graphene enhanced by elliptically polarized light excitation," *Science* **356**(6339), 736–738 (2017).
20. T. T. Luu and H. J. Wörner, "Measurement of the Berry curvature of solids using high-harmonic spectroscopy," *Nat. Commun.* **9**(1), 916 (2018).
21. T. T. Luu, V. Scagnoli, S. Saha, L. J. Heyderman, and H. J. Wörner, "Generation of coherent extreme ultraviolet radiation from  $\alpha$ -quartz using 50 fs laser pulses at a 1030 nm wavelength and high repetition rates," *Opt. Lett.* **43**(8), 1790–1793 (2018).
22. A. D. DiChiara, E. Sistrunk, T. A. Miller, P. Agostini, and L. F. DiMauro, "An investigation of harmonic generation in liquid media with a mid-infrared laser," *Opt. Express* **17**(23), 20959 (2009).
23. M. Ekimova, W. Quevedo, M. Faubel, P. Wernet, and E. T. Nibbering, "A liquid flatjet system for solution phase soft-x-ray spectroscopy," *Struct. Dyn.* **2**(5), 054301 (2015).
24. G. Galinis, J. Strucka, J. C. T. Barnard, A. Braun, R. A. Smith, and J. P. Marangos, "Micrometer-thickness liquid sheet jets flowing in vacuum," *Rev. Sci. Instrum.* **88**(8), 083117 (2017).
25. J. D. Koralek, J. B. Kim, P. Brůža, C. B. Curry, Z. Chen, H. A. Bechtel, A. A. Cordones, P. Sperling, S. Toleikis, J. F. Kern, S. P. Moeller, S. H. Glenzer, and D. P. DePonte, "Generation and characterization of ultrathin free-flowing liquid sheets," *Nat. Commun.* **9**(1), 1353 (2018).
26. T. T. Luu, Z. Yin, A. Jain, T. Gaumnitz, Y. Pertot, J. Ma, and H. J. Wörner, "Extreme-ultraviolet high-harmonic generation in liquids," *Nat. Commun.* **9**(1), 3723 (2018).
27. Z. Yin, T. T. Luu, and H. J. Wörner, "Few-cycle high-harmonic generation in liquids: in-operando thickness measurement of flat microjets," *JPhys Photonics* **2**(4), 044007 (2020).
28. P. Antoine, B. Carré, A. L'Huillier, and M. Lewenstein, "Polarization of high-order harmonics," *Phys. Rev. A* **55**(2), 1314–1324 (1997).
29. J. Levesque, Y. Mairesse, N. Dudovich, H. Pépin, J.-C. Kieffer, P. B. Corkum, and D. M. Villeneuve, "Polarization state of high-order harmonic emission from aligned molecules," *Phys. Rev. Lett.* **99**(24), 243001 (2007).
30. X. Zhou, R. Lock, N. Wagner, W. Li, H. C. Kapteyn, and M. M. Murnane, "Elliptically polarized high-order harmonic emission from molecules in linearly polarized laser fields," *Phys. Rev. Lett.* **102**(7), 073902 (2009).
31. H. Ruf, C. Handschin, R. Cireasa, N. Thiré, A. Ferré, S. Petit, D. Descamps, E. Mével, E. Constant, V. Blanchet, B. Fabre, and Y. Mairesse, "Inhomogeneous high harmonic generation in krypton clusters," *Phys. Rev. Lett.* **110**(8), 083902 (2013).
32. N. Klemke, O. D. Mücke, A. Rubio, F. X. Kärtner, and N. Tancogne-Dejean, "Role of intraband dynamics in the generation of circularly polarized high harmonics from solids," *Phys. Rev. B* **102**(10), 104308 (2020).
33. B. Schaefer, E. Collett, R. Smyth, D. Barrett, and B. Fraher, "Measuring the Stokes polarization parameters," *Am. J. Phys.* **75**(2), 163–168 (2007).
34. H. Höchst, P. Bulicke, T. Nelson, and F. Middleton, "Performance evaluation of a soft x-ray quadruple reflection circular polarizer," *Rev. Sci. Instrum.* **66**(2), 1598–1600 (1995).
35. C. von Korff Schmising, D. Weder, T. Noll, B. Pfau, M. Hennecke, C. Strüber, I. Radu, M. Schneider, S. Staack, C. M. Günther, J. Lüning, A. el dine Merhe, J. Buck, G. Hartmann, J. Viehhaus, R. Treusch, and S. Eisebitt, "Generating circularly polarized radiation in the extreme ultraviolet spectral range at the free-electron laser FLASH," *Rev. Sci. Instrum.* **88**(5), 053903 (2017).
36. T. Koide, T. Shidara, M. Yuri, N. Kandaka, K. Yamaguchi, and H. Fukutani, "Elliptical-polarization analyses of synchrotron radiation in the 5–80-eV region with a reflection polarimeter," *Nucl. Instrum. Methods Phys. Res., Sect. A* **308**(3), 635–644 (1991).
37. F. Schäfers, H.-C. Mertins, A. Gaupp, W. Gudat, M. Mertin, I. Packe, F. Schmolla, S. D. Fonzo, G. Soullié, W. Jark, R. Walker, X. L. Cann, R. Nyholm, and M. Eriksson, "Soft-x-ray polarimeter with multilayer optics: complete analysis of the polarization state of light," *Appl. Opt.* **38**(19), 4074 (1999).